

Magnetic frustration and glassiness in an icosahedral *i*-Tb-Cd quasicrystalFernand Denoel ^{1,*}, Deep Chandra Joshi ¹, Yu-Chin Huang,² Girma Hailu Gebresenbut,²
Cesar Pay Gómez,² and Roland Mathieu ^{1,†}¹*Department of Materials Science and Engineering, Uppsala University, Box 35, 751 03, Uppsala, Sweden*²*Department of Chemistry-Ångström Laboratory, Uppsala University, 751 21 Uppsala, Sweden*

(Received 26 February 2024; accepted 24 April 2024; published 13 May 2024)

The dynamical magnetic properties of the icosahedral *i*-Tb-Cd quasicrystal (QC) were investigated by means of squid magnetometry. At low temperatures, below $T \sim 4.5$ K, we observe conventional spin glass features including aging, memory, and rejuvenation. Interestingly, from $T \sim 4.5$ to 10 K, the spin configuration is also found to evolve with time (i.e., age as in spin glass), yet without memory. This suggests a reentrantlike behavior for the *i*-Tb-Cd QC, where upon cooling from high temperatures, the system first displays a magnetically frustrated phase before turning into a spin glasslike one at the lowest temperatures. We discuss the nature and possible origin of this magnetic behavior, in the light of the results obtained in the *i*-Gd-Cd QC, and ternary Tb-based quasicrystal approximants.

DOI: [10.1103/PhysRevB.109.184425](https://doi.org/10.1103/PhysRevB.109.184425)**I. INTRODUCTION**

Quasicrystals (QCs) constitute an intriguing state of matter where the building blocks are aperiodic along at least one dimension, but where the local atomic environments are perfectly well defined. Icosahedral quasicrystals (*i*-QCs) is the only type which is aperiodic along all three dimensions. In the case of the *R*-Cd Tsai-type series of *i*-QCs ($R = Y, Gd-Lu$), their structure can be described satisfactorily using a Tsai cluster elementary unit, a rhombic triacontahedron (RTH) with a unique atomic decoration described in Ref. [1], leaving acute rhombohedron (AR) and obtuse rhombohedron (OR) spaces that can also be described with a unique decoration, see Fig. 1. All Tsai clusters exhibit the same orientation throughout the structure, and are strictly only allowed to connect to the neighboring clusters by either sharing a face or by intersecting along their threefold axes, sharing an obtuse rhombohedron (OR), defining the icosahedral long-range order. In real Tsai QCs, most of the volume can be described by a network of interpenetrating Tsai clusters with same orientation and atomic decoration, surrounded by a few ORs and ARs with atomic decorations [1]. In the case where the rare-earth is trivalent, there is chemical disorder with Cd occupying partially the rare-earth sites. The atomic decoration of the RTHs can be separated in the Cd-only sites and mixed sites containing both Cd and rare-earths. In addition to forming an

icosahedron in each cluster, these mixed sites also exist for the stray ARs, with two nonequivalent sites, usually described as a double-Friauf polyhedron (DFP) with the surrounding Cd atoms. The building blocks and linkages are shown in Fig. 1. There exist 18 different local configurations for Tsai clusters to interconnect with their first neighbors, which gives a large variety of local geometries for the magnetic elements. Approximant crystals (ACs) are periodic crystals with similar local structure as the QCs [2] which can, hence, also be investigated to study the structure-property relationship in QCs. In some cases, the tetrahedra located in conventional Tsai clusters can be partially or totally replaced by a rare-earth ions [3,4]. In these intermetallic *R*-Cd systems, the magnetic *4f* elements interact through RKKY exchange, only dependent on the distance separating the magnetic ions. It is expected that the ferromagnetic-antiferromagnetic oscillating nature of the RKKY interaction as a function of distance, the multiple local atomic environments of *i*-QCs, and the fact that the first nearest neighbors of the magnetic quasiperiodic lattice of *i*-QCs are near identical [5,6] promotes magnetic frustration, favoring a spin glass state at low temperatures [7–9]. Spin glass states imply the appearance of short-range magnetic correlations at low temperature which collectively “freezes” the spin configuration in an out-of-equilibrium state, governed by slow spin dynamics [10]. Interestingly, spin glasses may occur as a result of either a mixture of ferromagnetic and antiferromagnetic interactions in the system, or by, e.g., a predominance of antiferromagnetic interactions over a magnetic lattice incompatible with antialigned first neighbors [11]. The spin glass behavior of the *i*-Gd-Cd QC has been demonstrated by magnetometry [7]. On the other hand, the *i*-Tb-Cd QC show ambiguous magnetization curves with regards to their previously mentioned spin freezing [12], with a significant irreversibility appearing above a broad cusp in the zero-field cooled (ZFC) magnetization. Interestingly, recent elastic and inelastic neutron scattering studies have evidenced short range

*fernand.denoel@angstrom.uu.se

†roland.mathieu@angstrom.uu.se

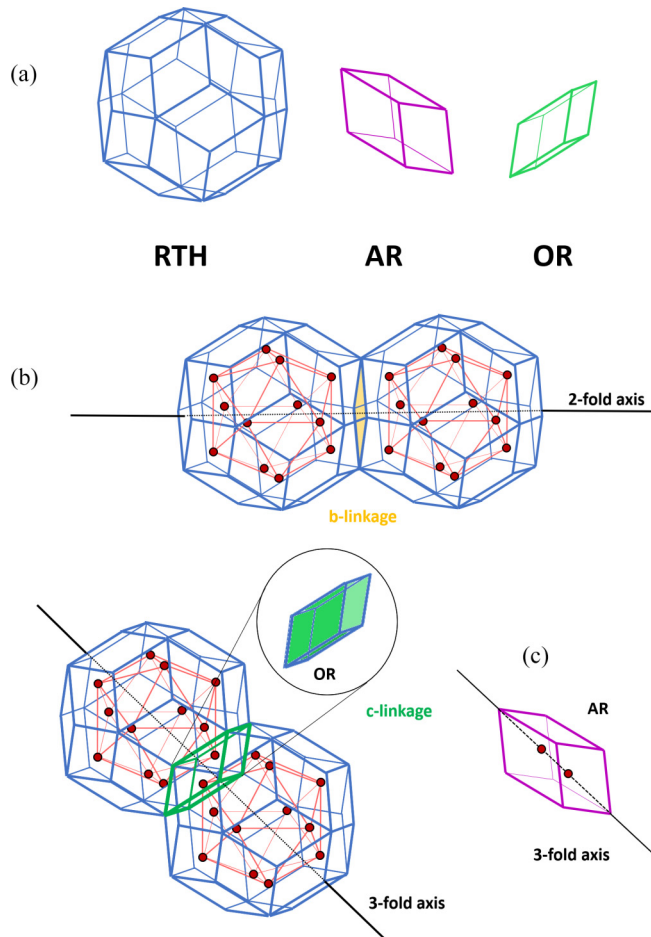


FIG. 1. (a) Building blocks of icosahedral quasiperiodic order. From left to right: rhombic triacontahedron (RTH), acute rhombohedron (AR), and obtuse rhombohedron (OR). (b) The two linkages rules that connect Tsai clusters and (c) the stray ARs separate from the Tsai clusters network, with two R inequivalent positions. The red spheres located in the RTH and stray AR represent the rare-earth positions.

magnetic correlation at temperatures above that of the ZFC cusp [13].

In the present paper, we have investigated in detail the dynamical magnetic properties and glassy state of i -Tb-Cd QC by means of magnetometry. The static magnetic properties of our QC are qualitatively and quantitatively similar to those reported earlier. We find that, unlike ordinary spin glasses and, e.g., the i -Gd-Cd QC which show a transition from a paramagnetic to a spin glass-like phase at low temperature, i -Tb-Cd QC displays an intermediate magnetically frustrated phase, which, e.g., shows aging but no memory features. We discuss in detail the nature and origin of this phase.

II. EXPERIMENTAL METHODS

A single crystal of the i -Tb-Cd QC was synthesized using the self-flux method. Similar conditions as reported by Goldman *et al.* [12] were used. In the present synthesis, elemental granules of Tb with purity 99.99 at.% and Cd with purity 99.999 at.% were used. A total mass of 2 g with starting

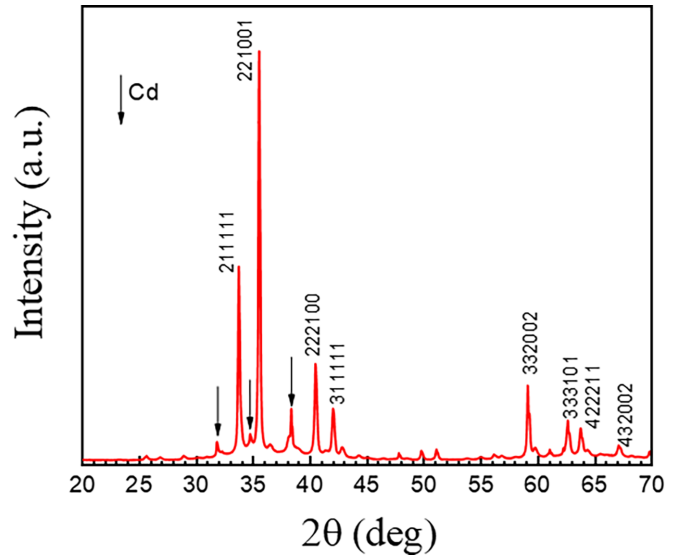


FIG. 2. Powder XRD pattern of the i -Tb-Cd QC; peaks from residual Cd flux are indicated with arrows.

nominal composition $\text{Tb}_{0.8}\text{Cd}_{99.2}$ was used. The starting materials were gathered in an alumina crucible, then sealed in a stainless steel ampule under Ar atmosphere, first heated to 700 °C and slowly cooled to 355 °C where the QC grains were separated from the Cd excess flux by centrifuging. i -Gd-Cd and i -Dy-Cd QCs were also synthesized using a similar method for comparison (see the Supplemental Material [14] and Ref. [7]). The phase purity and structural properties of the resulting sample were analyzed by x-ray powder diffraction (XPRD) using a Bruker D8 Powder diffractometer. The XPRD was measured from 2θ angle 20–70° with the step size 0.01. The indexed power pattern of i -Tb-Cd QC was characterized based on Ref. [15]. The magnetic properties, including the temperature-dependent zero field-cooled (ZFC), field-cooled (FC) magnetization, and ac susceptibility were acquired using a superconducting quantum interference design (SQUID) measurement system from Quantum Design Inc. Magnetic-field dependent magnetization measurements were recorded on the same equipment at a constant temperature ($T = 2$ K).

III. RESULTS AND DISCUSSION

The XRPD patterns displayed in Fig. 2 illustrates the phase purity of the QC sample, with the expected diffraction peaks from the i -Tb-Cd QC indexed. As sketched in Fig. 1, multiple local configurations exist in the i -Tb-Cd QC. The various local environment of magnetic elements appearing in QCs and ACs has been previously reported [6].

We note that since the relative concentration of Cd in the i -Tb-Cd QC is higher than the examples with no chemical disorder $M\text{Cd}_{5.7}$ QC for $M = \text{Yb}, \text{Ca}$, it is likely that Cd is present on the icosahedron shell of the Tsai cluster and the two DFP site, potentially up to saturation for the latter as the case in i -Gd-Cd [16]. The two R sites present on the DFP are closer than the edge length of the icosahedra sites [17], which may explain why these sites are more Cd rich than on the icosahedron, especially for large rare-earths.

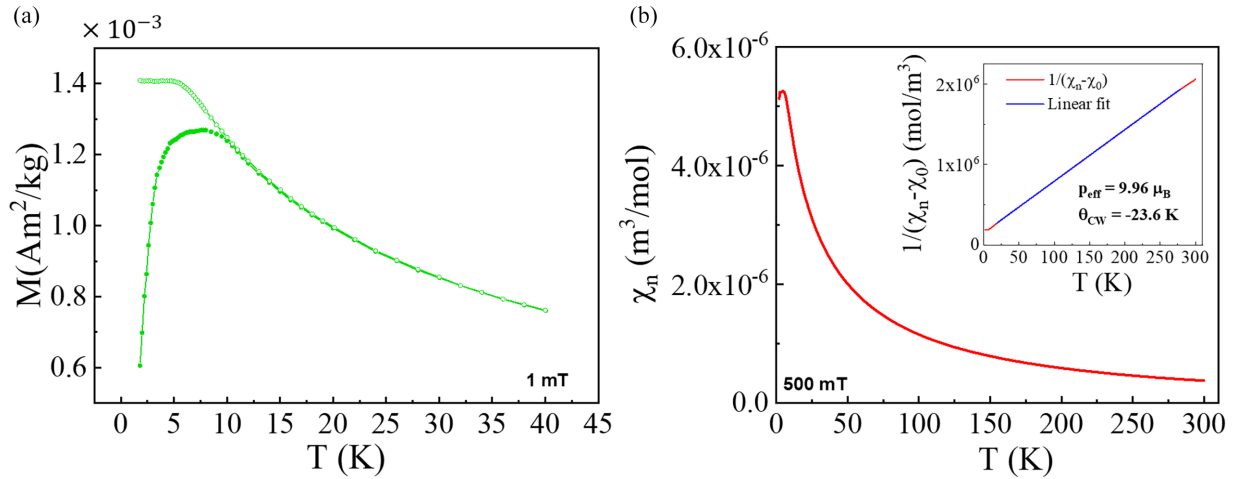


FIG. 3. (a) Zero-field cooled and field cooled magnetization curves of the *i*-Tb-Cd QC. (b) The dc magnetic susceptibility of the *i*-Tb-Cd QC recorded in a larger magnetic field. The inset shows the inverse susceptibility plotted as $1/(\chi_n - \chi_0)$ vs $T(\chi_0 = 1.1 \times 10^{-7} \text{ mol/m}^3)$, and linear fit.

Figure 3(a) shows the ZFC and FC magnetization recorded in a small magnetic field of 1 mT. No magnetic irreversibility is observed down to ~ 10 K, below which a rounded maximum is observed in the ZFC magnetization in the 5–7 K range. The present ZFC/FC curves are qualitatively and quantitatively similar to those reported earlier [12,18], namely a broad peak centered around 5.4 K and irreversibility below 8.7 K [12,18], and suggest a short-ranged magnetic order. Above 20 K, the magnetic susceptibility of the *i*-Tb-Cd QC recorded in higher magnetic fields follows a Curie-Weiss behavior [see Fig. 3(b)] with $\theta_{CW} = -23.6$ K, in quantitative agreement as well with the value $\theta_{CW} = -21$ K previously reported in Ref. [12]. This, in absolute values, is about four times the magnitude of the temperature of the broad maximum in the ZFC magnetization. The associated effective magnetic moment is $9.96 \mu_B$, which is the value expected for Tb, considering a $4f^8$ configuration and $J = 6$ value of Tb^{3+} , yielding $g\sqrt{J(J+1)}\mu_B = 9.72 \mu_B$. The *i*-Tb-Cd QC displays S-shaped $M(H)$ curves, with $M(\mu_0 H = 5\text{T}) \sim 3.3 \mu_B/\text{Tb}$, significantly lower than $gJ \mu_B = 9 \mu_B/\text{Tb}$ (see Fig. S3 of the SM). Owing to crystal electric field effects (CEF), it has been suggested that Tb could possess a local Ising-like spin orientation along the (icosahedral) crystal axes in *i*-Tb-Cd [19,20], with spins pointing either in or out from the mixed site icosahedron they are located on [13]. Associated to this complex magnetic state, short-range magnetic order was reported to develop at temperatures above the freezing temperature, considering neutron scattering data collected from 1.8 to 30 K [13]. The configurations on the icosahedron is reminiscent to the local spin configuration of pyrochlore spin ice, with a two-in two-out rule for spin configuration of the tetrahedra at low temperature [21].

Yamada *et al.* have demonstrated that doping of the non-magnetic Y in ACs at similar concentrations than the intrinsic dilution observed in QCs could suppress the antiferromagnetic long-ranged order in the TbCd_6 1/1 AC [16]. It is possible that, would all the rare-earth sites be occupied by Tb^{3+} ions, a long-ranged antiferromagnetic could exist in the *i*-Tb-Cd QC, but the disorder introduced by Cd dilution suppresses the

long-range order, converting it to a short-range order. Note that since the static magnetic properties of our *i*-Tb-Cd QC match not only qualitatively, but also quantitatively those of Goldman *et al.* [12], we assume a similar Cd content in our QC, yielding the chemical composition $\text{TbCd}_{7.69}$ [12].

The in-phase and out-of-phase components of the ac susceptibility of the *i*-Tb-Cd QC are shown in Fig. S2 of the SM. To be meaningful and reflect the intrinsic (linear) response of the system, the employed ac-excitation needs to be small; here 0.4 mT. Unfortunately, the obtained ac signal is too small to make quantitative assertions about the magnetic response, e.g., by scaling analysis [22]. Qualitatively, the ac susceptibility display an onset of irreversibility below 10 K (e.g., the appearance of frequency dependence in the in-phase component and an out-of-phase component) resembling that of spin glasses, which may be connected to the magnetic irreversibility observed in the ZFC/FC dc magnetization curves.

Spin glasses display aging, memory, and rejuvenation phenomena [11,23]. If a spin glass is rapidly cooled to a given temperature T_{halt} in the glassy phase in zero magnetic field, its microscopic spin configuration will rearrange itself over time, i.e., age. Interestingly, if a small magnetic field is applied after a certain time t_{halt} to record the intrinsic (linear) magnetic response of the material at that temperature, the obtained relaxation curves will show a dependence on t_{halt} , which reflects the age of the system being probed [11,24]. The aging is kept in memory unless the temperature is again changed from T_{halt} , inducing rejuvenation: the system appears young again, with a spin configuration reinitialized. Rejuvenation can be induced by resuming the cooling to a lower temperature as in an ordinary (reference) ZFC magnetization experiment. This shows that the time-dependent features of spin glasses such as aging, memory, and rejuvenation may be probed in temperature dependent experiments employing specific protocols, e.g., ZFC magnetization measurements recorded on reheating after including halts at constant temperatures (during which the aging takes place) in the initial cooling from the paramagnetic phase [24]. As a result of the rejuvenation

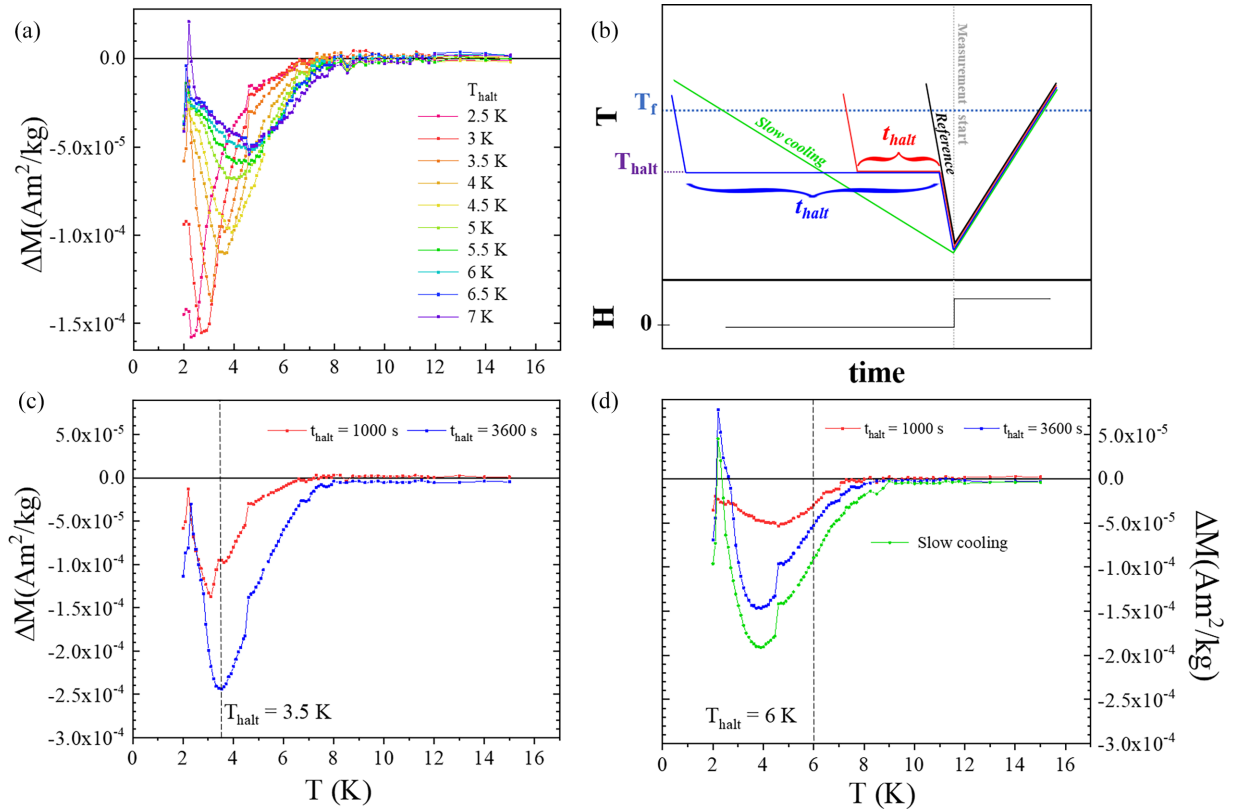


FIG. 4. (a) The results of memory experiments performed with $t_{\text{halt}} = 1000$ s at different temperatures T_{halt} in the range 2.5 K–7 K are shown in Fig. S4(a) in the SM (as M - T curves) and here as difference plots $\Delta M(T)$, obtained by subtracting the reference curve from each curve recorded after a halt. (b) Sketch of the change in temperature and applied magnetic field with time in the memory experiments: The ZFC magnetization is recorded on reheating after rapid and direct cooling down to the lowest temperature (“reference,” black curve) or after including halts (red and blue curves, illustrating halts of different durations). Another reference curve recorded after a slower cooling (0.2K/min) down to the lowest temperature is also depicted (green curve). (c), (d) The $\Delta M(T)$, plots for different halt times $t_{\text{halt}} = 1000$, 3600 s performed at $T_{\text{halt}} =$ (c) 3.5 K and (d) 6 K. The difference plot of a curve collected without halt, yet employing a slow cooling rate of (0.2 K/min) is added in (d) for comparison, with same color scheme as the sketch in (b).

phenomenon, the memory of the aging at a given temperature T_{halt} will appear in $M(T)$ curves as a dip centered around T_{halt} [7,24], more clearly shown as a ΔM difference plots obtained by subtracting a reference curve recorded without halt in the initial cooling from each of the curves recorded after a halt. These so-called dc memory experiments were employed to investigate the glassy features of the i -Gd-Cd QC [7].

Memory experiments are performed on the i -Tb-Cd QC using a waiting time $t_{\text{halt}} = 1000$ s for temperatures ranging from $T_{\text{halt}} = 2.5$ K to 7 K. The results are presented in Fig. 4(a) and Fig. S4 in the SM. The temperature dependence of the ZFC magnetization recorded after cooling with and without halt (reference curve) measured according to the protocol sketched in Fig. 4(b) is shown in Fig. S4(a) in the SM. Figure 4(a) shows the corresponding difference plots ΔM . The i -Tb-Cd QC displays clear ΔM memory dips centered in the vicinity of the respective T_{halt} for $T_{\text{halt}} < 4.5$ K, evidencing the aging, memory, and rejuvenation features of a spin glass and the i -Gd-Cd QC. However, in spin glasses and the i -Gd-Cd QC, memory dips centered near T_{halt} are observed at all T_{halt} up to the cusp temperature in the ZFC magnetization curve. In the i -Tb-Cd QC, memory diplike features are observed above 4.5 K up to the cusp temperature and above, however, broader in temperature and centered near ~ 5 K, independently of

T_{halt} . All the memory and memorylike curves become identical to the reference one above ~ 10 K, i.e., the irreversibility temperature.

To contrast further the dynamical behavior of the i -Tb-Cd QC below and above 4.5 K, the ΔM plots obtained at 3.5 K and 6 K for two halt times are shown in Figs. 4(c) and 4(d). In both cases, the (c) memory and (d) broad memorylike dips are larger when the halt is longer, as expected. However, as seen in Fig. 4(d), a broad memorylike dip centered at the same temperature may be obtained simply by subtracting the reference curve from a magnetization curve recorded, like the reference, without halt, yet employing a slower cooling rate during the initial cooling. This resembles the cooling rate effects observed in glassy systems [25], which suggests that in the temperature range ~ 4.5 –10 K the system exhibits aging, but no memory, as, e.g., the magnetically frustrated phases observed in reentrant systems, whose dynamical features (aging) are less robust to temperature changes [26]. The magnetization dips are broad and span the whole temperature range of irreversibility, i.e., from 10 K down to the lowest temperature, within which the spin configuration is continuously aging as the cooling proceeds [25].

The results may thus indicate that (antiferro)magnetic interactions are strongly frustrated in the i -Tb-Cd QC,

possibly geometrically, turning the material into a short-ranged magnetic phase below 10 K, yielding the observed short-range magnetic correlation recently uncovered in neutron experiments at temperatures above the broad cusp in ZFC magnetization [13]. In a reentrantlike fashion, this phase evolves into a spin glasslike one below 4.5 K.

Interestingly, a similar behavior was unraveled in a Tb ternary approximant system, Tb-Au-Si [27]. The pseudo-Tsai-type approximant (R atom at the center) show dynamical properties typical to those of spin glasses and the i -Gd-Cd QC, as well as the low-temperature ($T < 4.5$ K) phase of the i -Tb-Cd QC. Interestingly, the behavior of the regular Tsai-type approximant (no R atom at the center) suggests that a magnetically frustrated ferrimagnet phase is established at low temperature [27]. Namely, while temperature and magnetic field dependences suggest long-range ferrimagnetism for the Tsai phase, time-dependent data and memory experiments show that this ternary phase displays dynamical features, including aging, albeit no memory; a behavior akin to the “cooling rate dependent dips” observed here for i -Tb-Cd halts above 4.5 K [27].

It is unclear whether the i -Dy-Cd QC displays a similar behavior as the i -Tb-Cd QCs, owing to the small value of ΔM in this case, and limited range of temperature accessible, as seen in Fig. S5 of the SM. Yet it would be of interest to investigate in more detail the dynamical properties of other QCs such as the i - R -Cd QCs with $R = \text{Dy, Ho, Er, Tm}$, especially since the ZFC magnetization and specific heat curves of i - R -Cd QCs ($R = \text{Ho, Er, Tm}$) have a different behavior than the i -Gd-Cd and i -Tb-Cd QCs [28]. However, QCs using

lanthanide elements R with atomic number Z higher than Dy display transitions and/or features close to or below the lowest reachable temperature of conventional magnetometer. The different CEF associated to each R^{3+} may affect the spin configuration and long-range ordering in nontrivial ways, potentially differently than in the Tb^{3+} case, yet, the overall decrease of Cd dilution for smaller R^{3+} ions could promote antiferromagnetic long-range order if they are achievable on the icosahedral quasiperiodic lattice (cf the Cd content being $\text{GdCd}_{7.88}$ and $\text{TmCd}_{7.28}$ [12]).

IV. CONCLUSION

To conclude, we have investigated in detail the dynamical magnetic properties of a i -Tb-Cd QC by magnetometry. The ZFC memory experiments reveal that the system evolves from a paramagnet at high temperature to a magnetically frustrated short-ranged phase below 10 K where the system experiences aging independent of the halt temperature. Below 4.5 K, the magnetic behavior is similar to that of conventional spin-glasses, and the system displays aging, memory, and rejuvenation. We compare our results to the isostructural i -Gd-Cd QC and ternary Tb-based ACs. We speculate that the specific magnetic behavior of the i -Tb-Cd QC stems from crystal electric field effects and the strong geometrical frustration.

ACKNOWLEDGMENT

We thank the Knut and Alice Wallenberg Foundation (Grant No. KAW 2018.0019).

-
- [1] H. Takakura, C. P. Gómez, A. Yamamoto, M. De Boissieu, and A. P. Tsai, *Nat. Mater.* **6**, 58 (2007).
 - [2] A. Mori, H. Ota, S. Yoshiuchi, K. Iwakawa, Y. Taga, Y. Hirose, T. Takeuchi, E. Yamamoto, Y. Haga, F. Honda, R. Settai, and Y. Onuki, *J. Phys. Soc. Jpn.* **81**, 024720 (2012).
 - [3] G. Gebresenbut, T. Shiino, D. Eklöf, D. C. Joshi, F. Denoel, R. Mathieu, U. Häussermann, and C. Pay Gómez, *Inorg. Chem.* **59**, 9152 (2020).
 - [4] G. H. Gebresenbut, T. Shiino, M. S. Andersson, N. Qureshi, O. Fabelo, P. Beran, D. Qvarngård, P. Henelius, A. Rydh, R. Mathieu, P. Nordblad, and C. Pay Gomez, *Phys. Rev. B* **106**, 184413 (2022).
 - [5] Y. C. Huang, U. Häussermann, G. H. Gebresenbut, F. Denoel, and C. Pay Gómez, *Inorg. Chem.* **62**, 14668 (2023).
 - [6] F. Labib, D. Okuyama, N. Fujita, T. Yamada, S. Ohhashi, T. J. Sato, and A. P. Tsai, *J. Phys.: Condens. Matter* **32**, 415801 (2020).
 - [7] D. C. Joshi, G. Gebresenbut, C. Pay Gomez, and R. Mathieu, *Europhys. Lett.* **132**, 27002 (2020).
 - [8] T. Shiino, F. Denoel, G. H. Gebresenbut, D. C. Joshi, Y. C. Huang, C. P. Gómez, U. Häussermann, A. Rydh, and R. Mathieu, *Phys. Rev. B* **104**, 224411 (2021).
 - [9] F. Denoel, Y.-C. Huang, N. Kondedan, A. Rydh, C. Pay Gómez, and R. Mathieu, *Inorg. Chem.* **63**, 5040 (2024).
 - [10] P. E. Jönsson, R. Mathieu, P. Nordblad, H. Yoshino, H. A. Katori, and A. Ito, *Phys. Rev. B* **70**, 174402 (2004).
 - [11] P. Nordblad, *Phys. Scr.* **88**, 058301 (2013).
 - [12] A. I. Goldman, T. Kong, A. Kreyssig, A. Jesche, M. Ramazanoglu, K. W. Dennis, S. L. Bud'ko, and P. C. Canfield, *Nat. Mater.* **12**, 714 (2013).
 - [13] P. Das, A. Kreyssig, G. S. Tucker, A. Podlesnyak, F. Ye, M. Matsuda, T. Kong, S. L. Bud'ko, P. C. Canfield, R. Flint, P. P. Orth, T. Yamada, R. J. McQueeney, and A. I. Goldman, *Phys. Rev. B* **108**, 134421 (2023).
 - [14] See Supplemental Material at <http://link.aps.org/supplemental/10.1103/PhysRevB.109.184425> for more magnetometry results, including i -Gd-Cd and i -Dy-Cd QCs.
 - [15] V. Elser, *Phys. Rev. B* **32**, 4892 (1985).
 - [16] T. Yamada, H. Takakura, T. Kong, P. Das, W. T. Jayasekara, A. Kreyssig, G. Beutier, P. C. Canfield, M. De Boissieu, and A. I. Goldman, *Phys. Rev. B* **94**, 060103(R) (2016).
 - [17] T. Yamada, H. Takakura, H. Euchner, C. P. Gómez, A. Bosak, P. Fertey, and M. De Boissieu, *IUCrJ* **3**, 247 (2016).
 - [18] A. I. Goldman, *Sci. Technol. Adv.* **15**, 044801 (2014).
 - [19] S. Watanabe, *Proc. Natl. Acad. Sci. USA* **118**, e2112202118 (2021).
 - [20] S. Watanabe, *Sci. Rep.* **12**, 10792 (2022).
 - [21] M. Potts and O. Benton, *Phys. Rev. B* **106**, 054437 (2022).
 - [22] R. Mathieu, A. Asamitsu, Y. Kaneko, J. P. He, and Y. Tokura, *Phys. Rev. B* **72**, 014436 (2005).

- [23] H. Kawamura and T. Taniguchi, in *Handbook of Magnetic Materials*, edited by K. H. J. Buschow (Elsevier Ltd, Amsterdam, 2015), Vol. 24, pp. 1–436.
- [24] R. Mathieu, P. Jönsson, D. N. H. Nam, and P. Nordblad, *Phys. Rev. B* **63**, 092401 (2001).
- [25] E. Vincent, in *Ageing and the Glass Transition*, edited by M. Henkel, M. Pleimling, and R. Sanctuary (Springer, Berlin, Heidelberg, 2007), Vol. 716, pp. 7–60.
- [26] K. Jonason and P. Nordblad, *Eur. Phys. J. B* **10**, 23 (1999).
- [27] T. Shiino, F. Denoel, G. H. Gebresenbut, C. P. Gómez, P. Nordblad, and R. Mathieu, *Phys. Rev. B* **105**, L180409 (2022).
- [28] T. Kong, S. L. Bud'ko, A. Jesche, J. McArthur, A. Kreyssig, A. I. Goldman, and P. C. Canfield, *Phys. Rev. B* **90**, 014424 (2014).